ARTICLES
PUBLISHED ONLINE: 1 JUNE 2014 | DOI: 10.1038/NCHEM.1960
nature chemistry

Bulk protonic conductivity in a cephalopod structural protein

David D. Ordinario[1], Long Phan[1], Ward G. Walkup IV[1], Jonah-Micah Jocson[1], Emil Karshalev[1], Nina Hüsken[1] and Alon A. Gorodetsky[1,2]*

Proton-conducting materials play a central role in many renewable energy and bioelectronics technologies, including fuel cells, batteries and sensors. Thus, much research effort has been expended to develop improved proton-conducting materials, such as ceramic oxides, solid acids, polymers and metal–organic frameworks. Within this context, bulk proton conductors from naturally occurring proteins have received somewhat less attention than other materials, which is surprising given the potential modularity, tunability and processability of protein-based materials. Here, we report proton conductivity for thin films composed of reflectin, a cephalopod structural protein. Bulk reflectin has a proton conductivity of $\sim 2.6 \times 10^{-3}$ S cm^{-1} at 65 °C, a proton transport activation energy of ~0.2 eV and a proton mobility of $\sim 7 \times 10^{-3}$ cm^2 V^{-1} s^{-1}. These figures of merit are similar to those reported for state-of-the-art artificial proton conductors and make it possible to use reflectin in protein-based protonic transistors. Our findings may hold implications for the next generation of biocompatible proton-conducting materials and protonic devices.

Proton conduction is a ubiquitous and extensively studied fundamental phenomenon[1–20]. For example, a variety of chemical processes, including redox reactions and acid/base catalysis, are coupled to proton transfer[1–5]. In addition, numerous biomolecules, such as electrochemically driven proton pumps in mitochondria and voltage-gated proton channels in phagocytes, have evolved specific structural motifs that facilitate proton translocation[6–10]. Moreover, the function of an increasingly diverse array of technologically relevant devices, which include fuel cells, electrolysers, batteries and sensors, crucially relies on proton transport[11–17]. The study of proton conduction has therefore captured the attention of chemists, biologists and materials scientists for over 200 years[18–20].

Owing to the technological importance of proton conduction, solid-state proton-conducting materials, such as ceramic oxides, solid acids, polymers and metal–organic frameworks, remain the focus of much research effort[11–17]. Within this context, naturally occurring proteins have received less attention than other materials[11–17,21–26], which is surprising given the prevalence of proton translocation in biology[6–10]. Indeed, protein-based materials possess particular advantages as candidate proton conductors, including structural modularity, tunable physical properties, ease and specificity of functionalization, generalized expression/purification protocols and intrinsic biocompatibility[27–31]. Thus, naturally occurring proteins constitute a promising class of proton-conducting materials with a potential yet to be fully realized.

From an applications perspective, protein-based proton-conducting materials are uniquely positioned to contribute to the next generation of bioelectronics[32–36]. For example, given the importance of protons (and ions in general) for electrical signalling in biology[32–36], protonic transistors represent a natural choice for interfacing rugged traditional electronics and biological systems that are decidedly more fragile. One can envision the direct and robust transduction of biochemical events into electrical signals with such devices[32–36]. However, in spite of this potential for biological applications, there are few examples in the literature of protonic transistors (which include recent reports by Rolandi and co-workers of devices based on maleic chitosan)[37–42]. Protonic transistors from biological materials are therefore exciting targets for further research and development[32–36,40,41].

Given the significance of biologically compatible proton conductors, we chose to develop a new class of these materials from reflectin, a cephalopod structural protein[43–47]. Reflectins contain a large number of charged amino acid residues, consist of one to six highly conserved repeating subdomains separated by variable linker regions and possess little-to-no organized secondary structure[43–47]. Reflectins are also remarkably robust, even when exposed to acidic conditions, heated up to 80 °C or processed into films with standard lithographic protocols[47]. Moreover, within cephalopod skin cells (iridocytes), reflectins aggregate to form platelets, which play a crucial role in cephalopod structural coloration as part of modular Bragg reflector-like structures[48,49]. Our current studies were inspired not only by the favourable physical characteristics of reflectins, but also by the demonstration of electrical control over cephalopod skin iridescence, which hinted at the possibility of unique electrical behaviour for iridocyte proteins[50].

Herein, we describe the characterization of the conductive properties of platelet-like thin films from a *Doryteuthis* (formerly *Loligo*) *pealeii* reflectin A1 isoform[45–47]. Our studies show that bulk reflectin is an effective proton-conducting material. The protonic conductivities measured for reflectin's aggregated thin-film form (referred to hereafter as the solid state) are among the highest reported for naturally occurring proteins and are even comparable to those found for many state-of-the-art artificial proton conductors. Moreover, reflectin shows behaviour consistent with the Grotthuss mechanism of proton conduction and effectively exhibits the same electrical characteristics as a dilute acidic solution. Such favourable properties enable the demonstration of protonic transistors in which a protein (reflectin) serves as the active material. Our measurements indicate that reflectins may represent a promising new class of modular proton-conducting materials for bioelectronics and other applications.

[1]Department of Chemical Engineering and Materials Science, University of California, Irvine, Irvine, California 92697, USA, [2]Department of Chemistry, University of California, Irvine, Irvine, California 92697, USA. *e-mail: alon.gorodetsky@uci.edu

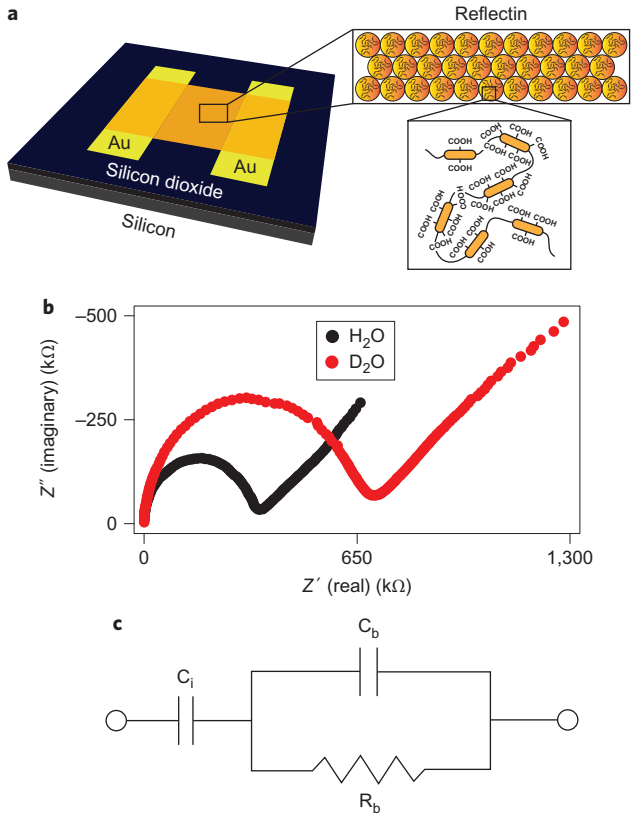

Figure 1 | Electrochemical impedance spectroscopy of reflectin films. **a**, Illustration of a two-terminal device in which a film composed of aggregated reflectin protein bridges two gold electrodes. Wild-type reflectin contains six repeating subdomains (orange) connected by variable linker regions (black). The carboxylic acid portions of the aspartic and glutamic acid residues in the repeating subdomains are labelled as COOH. The aliphatic portions of the labelled aspartic and glutamic acid residues are omitted for simplicity. **b**, A typical Nyquist plot for a reflectin-bridged two-terminal device in the presence of water vapour (black) and in the presence of deuterium oxide vapour (red), both at a RH of 90%. There is a change in the effective film resistance (the size of the semicircle increases) on switching from H_2O to D_2O. The device had a length of 50 μm, a width of 25,000 μm and a thickness of 4.6 μm. **c**, Diagram of the equivalent circuit used to analyse the impedance data. The circuit consists of a capacitor (C_i) in series with both a resistor (R_b) and a capacitor (C_b), which correspond to the film/electrode interface capacitance, the film bulk resistance and the film bulk capacitance, respectively.

Results

We began our studies by heterologously expressing a histidine-tagged *D. pealeii* reflectin A1 isoform in *Escherichia coli* (Supplementary Fig. 1). Reflectin A1 inclusion bodies were first prepared according to standard protocols[47]. The protein was then sequentially purified with immobilized metal-affinity chromatography under denaturing conditions and high-performance liquid chromatography (Supplementary Fig. 2)[47]. The identity of the purified reflectin was definitively confirmed by in-gel tryptic digestion and mass spectrometry (Supplementary Fig. 3)[47]. Our optimized protocol yielded >800 mg pure protein per litre of cell culture, which facilitated the preparation of reflectin films and subsequent electrical experiments[47].

For the electrical measurements, we fabricated two- and three-terminal bottom-contact devices, wherein reflectin served as the active material (Fig. 1 and Supplementary Fig. 4). In brief, we used shadow mask lithography to electron-beam evaporate arrays of paired gold (or palladium) electrodes onto either silicon dioxide/silicon (SiO_2/Si) or glass substrates. Subsequently, we drop-cast smooth and featureless thin films of reflectin directly onto these electrodes from aqueous solution and mechanically scribed away excess material, taking great care to avoid damaging the electrodes (Supplementary Fig. 4). The completed devices were then subjected to systematic electrical interrogation.

We first investigated the electrical properties of reflectin in a two-terminal configuration by recording current as a function of voltage, with gold electrodes serving as the electrical contacts on SiO_2/Si substrates. To avoid contributions from water electrolysis, we limited the maximum applied biases to ~1.5 V, which is the thermoneutral voltage for this reaction, and observed no evidence of gas formation for our devices; electrolysis would require even larger biases because of the probable presence of an overpotential[51,52]. Here, completely dry reflectin films at relative humidities (RHs) of <50% revealed current levels on the order of a few picoamps, which were similar to the current levels found in the absence of bridging material (Supplementary Fig. 5). However, at a high RH (90%), reflectin devices exhibited a marked increase in the current density to $0.6(\pm0.2) \times 10^{-2}$ A cm^{-2} at 1.5 V across a set of 16 independent films (Supplementary Fig. 5). The resulting current-versus-voltage characteristics displayed a clear deviation from linearity and hysteresis between the forward and reverse scans; this behaviour qualitatively resembled that found for maleic chitosan proton conductors contacted by blocking gold electrodes[40]. Such non-ideal characteristics indicated the presence of capacitive effects and/or charge-carrier blocking at the electrical contacts, consistent with protonic (and ionic) conductivity[53].

We sought to gain insight into whether reflectin's conductivity was protonic[6,10,36] or electronic[36,54–57] in origin (both types of mechanisms are well known for proteins). Long-range electronic conduction in proteins often occurs through hopping or tunnelling of charge carriers between suitably oriented peptides or cofactors that are readily oxidized or reduced[54,57]. Thus, we investigated the electrochemical properties of reflectin films in a standard three-electrode configuration with cyclic voltammetry. Our experiments revealed that reflectin on gold was electrochemically silent over a large potential window, with no distinct oxidation or reduction peaks (Supplementary Fig. 6). This lack of electrochemical activity at low potentials suggested that redox-associated electronic conduction might be improbable over long distances (tens of microns) for reflectin films.

To better understand the mechanism of conduction for reflectin, we used electrochemical impedance spectroscopy (EIS) to interrogate reflectin-based devices contacted with gold electrodes on glass substrates. We applied alternating current (a.c.) potentials to our hydrated films and visualized the real and imaginary parts of the impedance in Nyquist plots (Fig. 1)[58,59]. Our plots displayed a semicircle in the high-frequency region and an inclined spur in the low-frequency region. Such curves are a fingerprint of proton conductors contacted by blocking electrodes, in which the semicircle corresponds to the bulk protonic impedance and the spur corresponds to the pile-up of protons at the electrodes[58–62]. Thus, the curves were fit with a simple equivalent circuit, which has been shown to model proton-exchange membranes accurately by accounting for the bulk impedance and capacitive effects at the contacts (Fig. 1)[58–62]. The high quality of the fit indicated that this simple model was applicable for our reflectin films, and the equivalent circuit yielded a bulk resistance that translated into an effective conductivity of $1.0(\pm0.5) \times 10^{-4}$ S cm^{-1} across a set of nine independent films. These EIS measurements implied that protonic conductivity was probable for our material.

As additional evidence for proton conduction in reflectin films, we sought to observe the kinetic isotope effect for our two-terminal devices. To this end, we recorded EIS measurements for reflectin films contacted with gold electrodes on glass in the presence of

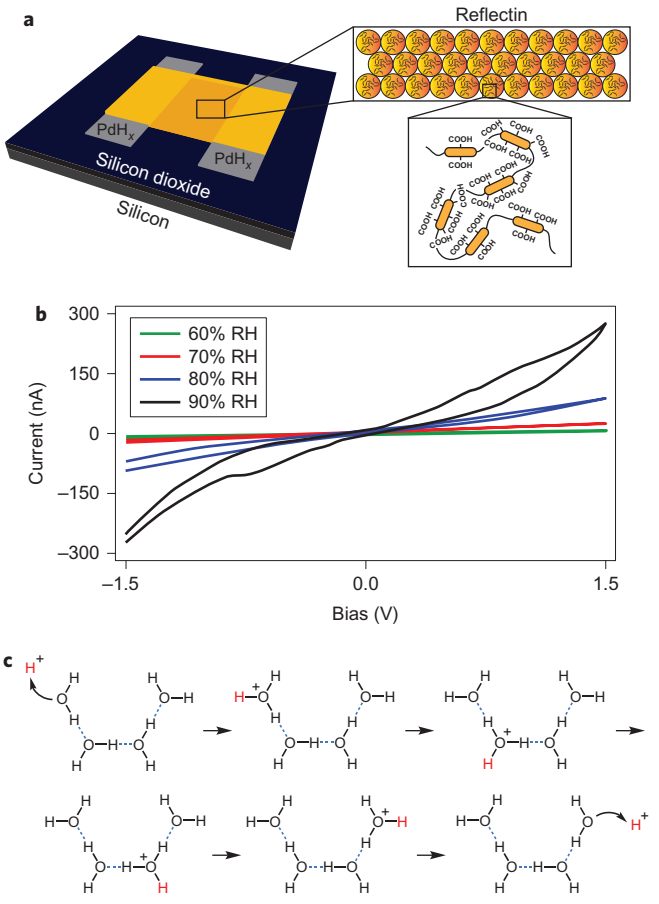

Figure 2 | Electrical properties of reflectin films contacted with palladium hydride electrodes. a, Illustration of a two-terminal device in which a film composed of aggregated reflectin protein bridges two PdH_x electrodes. **b**, The electrical response (current versus voltage) of reflectin films contacted with PdH_x electrodes. The current increases as the RH is raised from 60% to 90%. Both the forward and reverse scans are shown for each measurement. The device had a length of 50 μm, a width of 220 μm and a thickness of 1.3 μm. **c**, Illustration of proton translocation along a chain of hydrogen-bonded water molecules, as postulated to occur for the Grotthuss mechanism. The mobile proton that moves along the hydrogen-bonded chain is labelled in red.

deuterium oxide (D_2O) vapour. At RHs of 90%, the solvent uptake of D_2O was almost identical to that of H_2O for reflectin, which ensured a reliable comparison (Supplementary Table 1). Here, we observed a distinct isotope effect, in close agreement with literature observations for other proton-conducting materials[11–16,53]; on going from H_2O to D_2O *in situ*, the Nyquist plots showed identical characteristic inclined spurs, but the conductivity decreased by 40% from $1.0(\pm0.5) \times 10^{-4}$ S cm^{-1} to $0.6(\pm0.3) \times 10^{-4}$ S cm^{-1} across a set of nine independent films (Fig. 1). This measurement was again consistent with proton conduction in reflectin films.

We proceeded to investigate the electrical properties of reflectin films when contacted with proton-transparent palladium hydride (PdH_x) electrodes (Fig. 2). PdH_x facilitates proton injection to yield higher currents for proton-conducting materials (and lower currents for electron-conducting materials)[40,63]. We therefore fabricated two-terminal devices with Pd as the electrode material and exposed these devices to H_2 gas, which enabled the formation of PdH_x electrical contacts *in situ*[40,63]. At a RH of 90%, electrical measurements for such devices yielded a current density of $8.2(\pm5.9) \times 10^{-2}$ A cm^{-2} at 1.5 V across a set of 16 independent films (Fig. 2); the spread in the current densities probably resulted from variability among the non-stoichiometric PdH_x contacts. Although the current densities were over an order of magnitude higher than those found for gold electrodes, the reflectin films did not appear to degrade as a result of electrical interrogation, as gauged by optical microscopy (Supplementary Fig. 7). If significant film degradation had occurred, it might have been accompanied by permanent changes in film coloration. In addition, the current–voltage curves displayed hysteresis consistent with charge accumulation/depletion at the contacts (Fig. 2)[40,53], but relative to devices with gold electrodes, the hysteresis was somewhat reduced, presumably as a result of the improved charge injection. These observations supported the notion of proton conduction in reflectin films.

We also explored the properties of reflectin films contacted with PdH_x electrodes at different levels of hydration. Previous studies have demonstrated that reflectin effectively behaves as a hydrogel, swelling as a function of RH[44,45,47]. Here, our reflectin devices displayed a noticeable increase in the current level with increasing humidity (Fig. 2). For biomolecular proton conductors, water uptake induces the formation of hydrogen-bonded proton-conduction pathways, which facilitate Grotthuss-type proton transfer[10,18–20,40] (Fig. 2). Given the large number of charged and/or hydrophilic residues found in reflectin[44,45,47], the same effect probably accounted for our observed increase in current as a function of RH. Taken together, our measurements with PdH_x contacts suggested that bulk reflectin was a proton-conducting material.

To gain insight into the structural origins of reflectin's conductive properties, we leveraged reflectin's advantages as a protein-based material and introduced targeted mutations within its primary sequence. Reflectin's polar charged amino acid side chains (aspartic acid, glutamic acid, lysine, arginine and histidine) probably play a crucial role in proton transport, as observed for other proteins[6,8,10]. For example, the carboxylic acids on its aspartic (D) and glutamic (E) amino acid residues (pK_a values of 3.9 and 4.3, respectively)[64] may either participate in hydrogen bonding or donate the excess protons necessary for conductivity in hydrated reflectin[6,8,10]; eliminating the residues that contain carboxylic acid should therefore decrease reflectin's protonic conductivity. To test this hypothesis, we heterologously expressed and purified a reflectin mutant (termed DE->A), in which all of the aspartic acid and glutamic acid residues were substituted with alanine (Fig. 3 and Supplementary Figs 8 and 9). Despite the removal of hydrophilic aspartic and glutamic acid residues, the DE->A mutant exhibited a similar water uptake to that of wild-type reflectin (Supplementary Table 1), presumably because of the overall large percentage of charged residues in reflectin (Supplementary Fig. 1). Our PdH_x devices fabricated from the DE->A mutant featured a current density of $0.9(\pm0.2) \times 10^{-2}$ A cm^{-2} at 1.5 V across a set of 11 independent films, which was approximately an order of magnitude lower than that found for wild-type reflectin (Fig. 3). This measurement further corroborated the notion of protonic conductivity for bulk reflectin.

To better understand the conductive behaviour of reflectin, we also altered its amino acid sequence dramatically. Reflectin's multiple conserved repeating subdomains and self-assembly properties suggest that this protein possesses a defined quaternary structure/nanoscale morphology in the solid state[43–47]. We suspect that this potentially unique structure/morphology enables the formation of hydrogen-bonded water networks, which facilitate effective Grotthuss-type proton transfer. Consequently, we postulated that scrambling the primary sequence of reflectin to eliminate the conserved subdomains should disrupt the protein's structure and, in turn, decrease its conductivity by impeding the formation of the requisite hydrogen-bonded water networks[10,18–20,40]. To test this hypothesis, we heterologously expressed and purified a reflectin mutant (termed Random) in which the amino acid order was scrambled, but the percentage of the individual amino acids

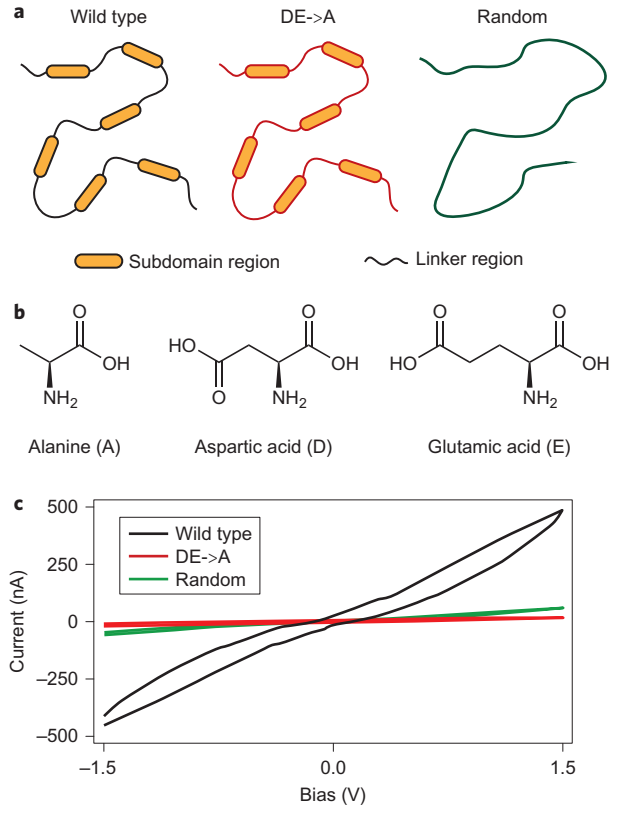

Figure 3 | Comparison of the electrical properties of wild-type and mutant reflectins. a, Cartoon of the primary structures of wild-type reflectin (left), the DE->A mutant (centre) and the Random mutant (right). The wild-type and DE->A mutant reflectin consist of six repeating subdomains (orange) connected by linker regions (coloured black for wild type and red for DE->A). For the DE->A mutant, the aspartic and glutamic acids have been replaced by alanine. For the Random mutant (green), the amino acid sequence has been scrambled to eliminate the repeating subdomains. **b**, Illustration of the chemical structures of alanine (A), aspartic acid (D) and glutamic acid (E). **c**, Comparison of the typical electrical characteristics (current versus voltage) for PdH_x electrode two-terminal devices fabricated from wild-type reflectin (black), the DE->A mutant (red) and the Random mutant (green). The current for the mutants decreases relative to that for the wild-type protein. Both the forward and reverse scans are shown for each measurement. The RH was 90%. The wild-type, DE->A mutant and Random mutant devices had lengths of 50, 50 and 50 μm, respectively, widths of 265, 210 and 220 μm, respectively, and thicknesses of 0.8, 1.0 and 1.1 μm, respectively.

(including the D and E residues) was maintained (Fig. 3 and Supplementary Figs 10 and 11). Although the Random mutant exhibited a similar water uptake to that of wild-type reflectin (Supplementary Table 1), PdH_x devices fabricated from this variant featured a current density of $1.7(\pm0.3) \times 10^{-2}$ A cm^{-2} at 1.5 V across a set of 11 independent films, which was approximately fivefold lower than that measured for wild-type reflectin (Fig. 3). Interestingly, the current density of the Random mutant was twofold higher than the current density of the DE->A mutant, potentially a result of the Random mutant's higher aspartic and glutamic amino acid content. Overall, our observations supported the notion that residues containing carboxylic acid play proton-donation or hydrogen-bonding roles for reflectin and underlined the probable importance of reflectin's structural features for its electrical properties.

We sought to characterize further the protonic conductivity in our films by interrogating them with EIS as a function of temperature. We therefore formulated Nyquist plots for reflectin devices contacted with blocking gold electrodes on glass over a temperature range from 30 °C to 65 °C (Fig. 4); reflectin is expected to be stable across this range because it maintains its functionality even after processing at temperatures as high as 80 °C (ref. 47). By fitting the impedance data with the equivalent circuit depicted in Fig. 1, we determined the conductivity of our reflectin films at different temperatures (Fig. 4). At a RH of 90% and a temperature of 65 °C, we measured a peak conductivity of 2.6×10^{-3} S cm^{-1} and an average conductivity of $1.2(\pm1) \times 10^{-3}$ S cm^{-1} across a set of three independent films (Fig. 4). These values compare favourably to those found for other proton-conducting materials[11–17] and are among the best reported for any bulk solid-state material from a naturally occurring protein[21–26].

We next constructed Arrhenius-type conductivity plots from our temperature-dependent measurements, which allowed us to determine the activation energy (E_a) of proton conduction for reflectin (Fig. 4)[12,53]. This activation energy corresponds to the cost of dissociating and/or transporting protons through the hydrogen-bonded water networks that presumably permeate our protein films[10,20]. The average value of $E_a = 0.22(\pm0.05)$ eV calculated from a linear fit of our measurements was characteristic of a Grotthuss-type conduction mechanism (Fig. 2)[10,19,20]; similar activation energies have been found for proton conduction in gramicidin channels

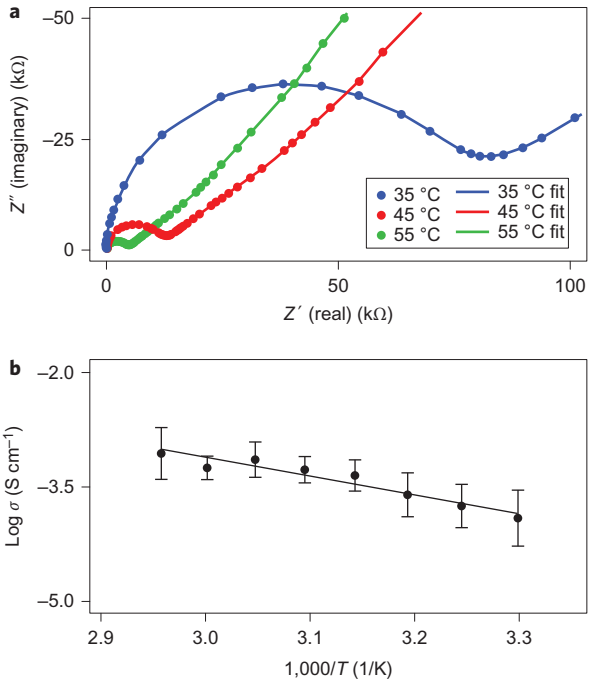

Figure 4 | Electrochemical impedance spectroscopy of reflectin films as a function of temperature. a, Typical Nyquist plots of the imaginary part of the impedance (Z'') versus the real part of the impedance (Z') for a gold electrode two-terminal reflectin device at a RH of 90%. The impedance responses were recorded at temperatures of 35 °C (blue dots), 45 °C (red dots) and 55 °C (green dots). For each temperature, the lines represent a fit of the data with an equivalent circuit model, which accounts for the bulk impedance and capacitive effects at the gold contacts. The device had a length of 100 μm, a width of 25,000 μm and a thickness of 2.6 μm. **b**, Arrhenius-type plot of the conductivity (σ) as a function of temperature for reflectin devices at a RH of 90%. The measurements were performed at 5 °C intervals over a temperature range of 30 °C to 65 °C, with each data point corresponding to three independent films. The line represents a linear fit of the data. The error bars represent the standard deviation for each data point.

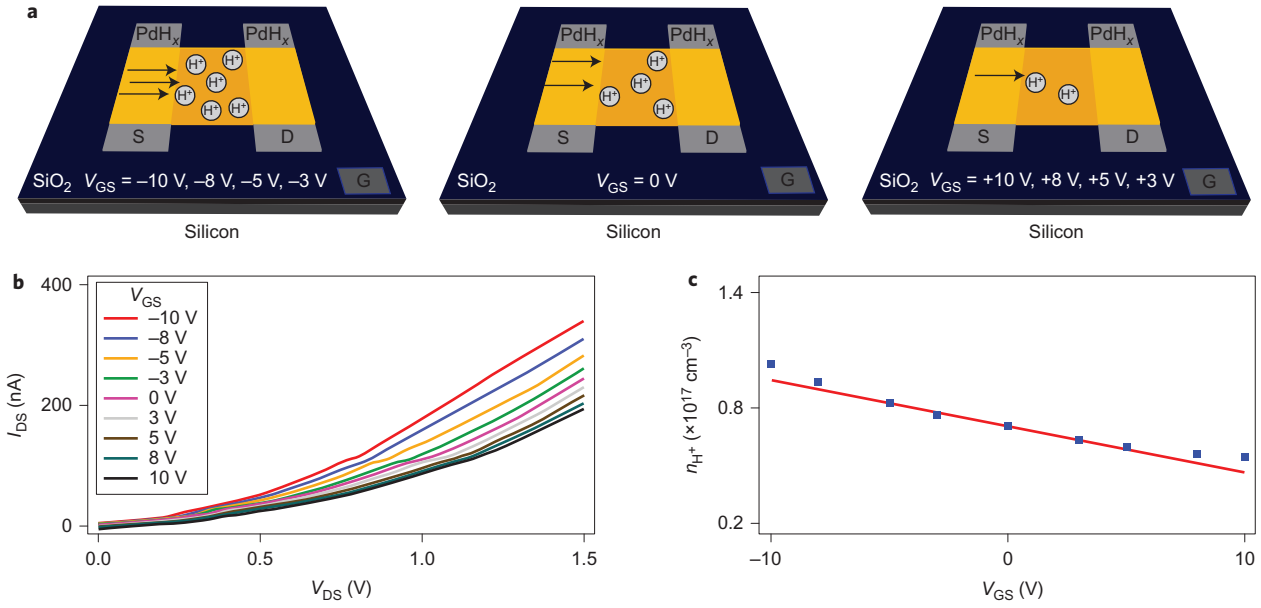

Figure 5 | Electrical characteristics of protonic transistors from reflectin. a, Illustration of the proton current for a reflectin-bridged three-terminal protonic transistor under different applied gate voltages (V_{GS}). The current decreases on moving from a negative gate voltage (left) to a gate voltage of zero (middle) to a positive gate voltage (right). The device is fabricated on a SiO_2/Si substrate with PdH_x electrodes as the electrical contacts. **b**, Typical source–drain current (I_{DS}) as a function of the source–drain voltage (V_{DS}) at different values of V_{GS}. The magnitude of I_{DS} increases as V_{GS} is modulated from positive to negative values. The measurements were performed at a RH of 90%. The device has a length of 50 μm, a width of 267 μm and a thickness of 1.1 μm. **c**, Plot of the experimentally observed charge-carrier density (proton concentration) as a function of V_{GS} (blue squares). The data are derived from the current–voltage curves in **b** for this specific device. The red line represents the theoretically expected change in the proton concentration, as determined from the equation $n_{H^+} = n_{H^+}{}^0 - V_{GS}C_{GS}/et$ (where n_{H^+} is the proton concentration at an arbitrary gate bias and $n_{H^+}{}^0$ is the experimentally observed proton concentration at $V_{GS} = 0$ V). There is agreement between the observed and expected modulations of the charge-carrier density.

($E_a \approx 0.2 \sim 0.3$ eV) and dilute acids ($E_a \approx 0.1$ eV)[10,19,20]. The low activation energy provided additional confirmation of protonic conductivity for bulk reflectin.

Given that proton conductors are important for a variety of high-technology applications[11–17], we sought to demonstrate the utility of reflectin in a technologically relevant device. We chose to focus our efforts on the fabrication of protonic transistors because only a handful of these have been reported, none of which used a naturally occurring protein as the active material[37–42]. We therefore fabricated three-terminal reflectin devices that featured PdH_x electrical contacts (formed *in situ*) on SiO_2/Si substrates; the PdH_x contacts enabled the selective injection of protons into our films[40,63].

We proceeded to study the electrical properties of our reflectin-based transistors. Thus, we recorded the protonic current between the source and the drain (I_{DS}) as a function of the applied voltage between the source and the drain (V_{DS}), at the same time as modulating the gate voltage (V_{GS}) (Fig. 5). Our measurements demonstrated electrostatic control over proton conduction: a negative V_{GS} induced the injection of protons into the channel, which increased the observed current, and a positive V_{GS} depleted the channel of protons, which decreased the observed current (Fig. 5). The electrostatic gating effects were remarkably reproducible, as exemplified by curves obtained from four representative devices (Fig. 5 and Supplementary Fig. 12). For low source–drain biases, we observed a small barrier for current flow, probably associated with the activation energy of proton dissociation/transport. Furthermore, in agreement with previous measurements, the I_{DS} versus V_{DS} curves exhibited hysteresis, presumably caused by charge accumulation/depletion at the contacts or an imperfect reflectin/SiO_2 interface (Supplementary Fig. 13)[40]. We also recorded negligible leakage currents, as might be expected for a proton-conducting active material on a proton-insulating substrate (Supplementary Fig. 14). Altogether, our findings demonstrated the functionality of reflectin in protonic transistors.

As a consistency check, we compared the conductivities calculated from our transistor measurements with the values determined by EIS. The slope of the I_{DS} versus V_{DS} plot at $V_{GS} = 0$ V yielded an effective resistance for the reflectin films, which translated into a conductivity of $1.1(\pm 0.3) \times 10^{-4}$ S cm^{-1} for seven independent devices. This value was similar to the conductivity of $1.0(\pm 0.5) \times 10^{-4}$ S cm^{-1} found with EIS (Fig. 1). Given the substantial experimental differences between the two techniques, this agreement highlights the robustness and reliability of our measurements.

We next estimated the effective proton mobility from the transfer characteristics of our devices via a literature protocol[41]. Thus, we extracted the conductivity of our films from the I_{DS} versus V_{DS} curves at different V_{GS} biases (Fig. 5). Linear fits of the dependence of the conductivity on V_{GS} yielded a mobility of $\mu_{H^+} = 7.3(\pm 2.8) \times 10^{-3}$ cm^2 V^{-1} s^{-1} for seven independent devices. This value is in agreement with mobilities reported for proton conduction in dilute acid solutions ($\sim 3 \times 10^{-3}$ cm^2 V^{-1} s^{-1})[20], PEDOT:PSS ($\sim 3.9 \times 10^{-3}$ cm^2 V^{-1} s^{-1})[65] and maleic chitosan proton conductors ($\sim 4.9 \times 10^{-3}$ cm^2 V^{-1} s^{-1})[40].

Finally, we evaluated the charge-carrier density in our reflectin films. From the equation $\sigma_{H^+} = \mu_{H^+} n_{H^+} e$ (where σ_{H^+} is the proton conductivity and e is the elementary charge) and our calculated mobility, the free proton concentration was estimated to be $n_{H^+} = 10.6(\pm 6.1) \times 10^{16}$ cm^{-3} at $V_{GS} = 0$ V for seven independent devices[40,41]. These excess protons may originate from reflectin's many charged residues, such as the D and E amino acids that contain carboxylic acid. Moreover, from our I_{DS} versus V_{DS} curves, we determined the change in the number of free protons on the application of different gate biases (Fig. 5). The experimentally observed proton concentrations were in excellent agreement with those predicted theoretically by the equation $n_{H^+} = n_{H^+}{}^0 - V_{GS}C_{GS}/et$ (where C_{GS} is the gate capacitance per

unit area and t is the film thickness), which further underlines the consistency of our measurements (Fig. 5 and Supplementary Fig. 12)[40].

Discussion

We have discovered and characterized novel electrical properties for the cephalopod structural protein reflectin. The protein was interrogated by humidity-dependent direct current (d.c.) electrical measurements with both proton-blocking and proton-injecting contacts, a.c. electrical measurements in the presence of water and deuterium oxide, rationally guided mutagenesis experiments and temperature-dependent EIS. Our findings indicate that reflectin functions as an efficient proton-conduction medium.

Based on our measurements, we infer that reflectin exhibits the characteristics of a dilute acid, with an average proton conductivity of $\sim 1 \times 10^{-4}\,S\,cm^{-1}$, a proton transport activation energy of $\sim$0.2 eV and a proton mobility of $\sim 7 \times 10^{-3}\,cm^2\,V^{-1}\,s^{-1}$. Bulk reflectin is quite unique in this regard; as far as we are aware, no other protein has been shown to mimic a dilute acidic solution so closely. Moreover, reflectin's maximum conductivity of $2.6 \times 10^{-3}\,S\,cm^{-1}$ at 65 °C is among the largest values found for any naturally occurring protein. Within the context of other biological (and even artificial) proton-conducting materials, reflectin's figures of merit are impressive and may represent new benchmarks for proteins in the solid state[21–26].

Reflectin's physical properties enable the fabrication and characterization of protein-based protonic transistors. The characteristics of our transistors are similar, in terms of mobility, threshold voltage and on/off current ratio, to those reported previously for devices based on maleic chitosan[40]. However, relative to maleic chitosan, reflectin allows protonic transistors to leverage the distinct advantages of protein-based materials, which include structural modularity, tunable physical properties, ease and specificity of functionalization, and generalized expression/purification [27–31]. Indeed, reflectin is simple to produce in high purity and yield, stable under harsh conditions and amenable to modulation of its electrical properties through site-directed mutagenesis. Consequently, given the handful of reported examples of protonic transistors and the possibilities available to functional protein-based materials, our reflectin-based devices may offer exciting new research avenues.

Here, it is important to underline our device reliability and consistency. Electrical measurements are known to be notoriously difficult for delicate protein-based systems, which are often unstable and undergo degradation[6,10,36,52–54]. However, reflectin films withstand processing and electrical cycling under acidic conditions and at elevated temperatures. Moreover, our electrochemical impedance studies and transistor measurements are in good agreement with one another. Our observations thus highlight the robustness of reflectin as a candidate material for bioelectronic devices.

Reflectin's function as a proton-conducting material is especially fascinating when one considers its unique amino acid sequence, which contains $\sim$30% hydrophilic charged residues and $\sim$20% hydrophobic aromatic residues (Supplementary Fig. 1)[43–47]. This unusual sequence composition makes reflectin amphipathic and induces its aggregation into nanoparticles both in solution and in thin films[44,45,47]. We postulate cautiously that hydrated reflectin films are segregated into distinct hydrophobic regions and proton-conducting hydrophilic water channels, which probably serve as highly effective conduits for proton transport. Interestingly, this type of segregated structure would be directly analogous to that reported for the sulfonated fluoropolymer Nafion[14]. Our mutagenesis studies and electrical experiments, together with previous characterization of reflectin films[45], provide compelling evidence that reflectin may possess well-defined and potentially unique morphology/structural features in the hydrated solid state. The exact internal structure of reflectin films probably holds the key to understanding this protein's unexpected electrical properties and certainly represents a fruitful area for further exploration. Our observations thus hint that reflectin may constitute a template for the design and production of the next generation of biologically compatible proton-conducting materials.

Methods

Preparation of wild-type and mutant reflectins. Wild-type reflectin A1 was prepared according to the previously reported literature protocols detailed in Supplementary Sections I, II and III[47]. The genes coding for the DE->A and Random reflectin mutants were designed, synthesized and cloned as described in Supplementary Section I. The mutant reflectins were expressed, purified and characterized in identical fashion to wild-type reflectin A1, as outlined in Supplementary Sections II and III.

Fabrication of reflectin devices. Two- and three-terminal devices were fabricated on either glass or SiO_2/Si substrates. Prior to device fabrication, the SiO_2/Si substrates were cleaned in Piranha solution, and the glass substrates were cleaned by sequential sonication in acetone and isopropanol. Next, arrays of paired electrodes that consisted of a 4 nm chromium adhesion layer overlaid with either a 40 nm gold or a 40 nm palladium layer were electron-beam evaporated onto the clean substrates through a shadow mask. The devices were completed by drop-casting an aqueous reflectin solution directly onto the electrode patterns, and the resulting films were allowed to dry in air overnight. Subsequently, excess material was scribed away mechanically to leave a rectangular reflectin film between each pair of electrodes. To form proton-injecting PdH_x electrodes, arrays of palladium electrodes were exposed to a 5% hydrogen/95% argon atmosphere *in situ*. Additional details of the device fabrication procedures are provided in Supplementary Section IV.

Physical characterization of reflectin devices. The reflectin devices were characterized with optical microscopy and atomic force microscopy. The length and width of the reflectin films were determined by analysis of optical images obtained with a Zeiss Axio Imager A1 Microscope. The thicknesses of both dry and humidified reflectin films were determined through the analysis of topographical scans obtained with an Asylum Research MFP-3D Atomic Force Microscope outfitted with an Asylum Research Humidity Sensing Cell. Additional details of the physical characterization procedures are provided in Supplementary Section V.

Electrical characterization of reflectin devices. The completed devices were characterized electrically in multiple distinct configurations. For two- and three-terminal d.c. measurements on SiO_2/Si substrates, the current was recorded as a function of voltage on a Cascade Microtech PM-5 Probe Station outfitted with an Agilent 4156C Semiconductor Parameter Analyzer. For three-terminal measurements with PdH_x electrodes, the source–drain current was recorded as a function of the source–drain voltage at variable applied gate voltages. For two-terminal a.c. measurements on glass substrates, the impedance data were collected on either a Hewlett Packard 4192A LF Impedance Analyzer or an Agilent 4294A Impedance Analyzer. The humidity was monitored constantly with a hygrometer during all electrical experiments. Additional details of the electrical characterization procedures are provided in Supplementary Section VI.

Analysis of the electrical data. The figures of merit for reflectin devices were extracted from analysis of the current versus voltage characteristics and impedance data. The relevant calculations are described in Supplementary Section IX.

Received 23 June 2013; accepted 16 April 2014; published online 1 June 2014

References

1. Caldin, E. F. & Gold, V. *Proton-Transfer Reactions* (Chapman and Hall, 1975).
2. Müller, A., Ratajczak, H., Junge, W. & Diemann, E. *Electron and Proton Transfer in Chemistry and Biology: Studies in Physical and Theoretical Chemistry* Vol. 78 (Elsevier, 1992).
3. Karlin, K. D., Kramarz, K. W. & Norton, J. R. *Slow Proton-Transfer Reactions in Organometallic and Bioinorganic Chemistry* (Wiley, 1994).
4. Douhal, A., Lahmani, F. & Zewail, A. H. Proton-transfer reaction dynamics. *Chem. Phys.* **207,** 477–498 (1996).
5. Weinberg, D. R. *et al.* Proton-coupled electron transfer. *Chem. Rev.* **112,** 4016–4093 (2012).
6. Schulten, Z. & Schulten, K. Proton conduction through proteins: an overview of theoretical principles and applications. *Methods Enzymol.* **127,** 419–438 (1986).
7. DeCoursey, T. E. Voltage-gated proton channels and other proton transfer pathways. *Physiol. Rev.* **83,** 475–579 (2003).
8. DeCoursey, T. E. Voltage-gated proton channels: what's next? *J. Physiol.* **586,** 5305–5324 (2008).
9. Gensch, T., Heberle, J. & Viappiani, C. Proton transfer in biological systems. *Photochem. Photobiol.* **5,** 529–530 (2006).

10. Wraight, C. A. Chance and design – proton transfer in water, channels, and bioenergetics processes. *Biochim. Biophys. Acta* **1757,** 886–912 (2006).
11. Colomban, P. *Proton Conductors: Solids, Membranes and Gels – Materials and Devices* (Cambridge Univ. Press, 1992).
12. Kreuer, K.-D. Proton conductivity: materials and applications. *Chem. Mater.* **8,** 610–641 (1996).
13. Kreuer, K.-D., Paddison, S. J., Spohr, E. & Schuster, M. Transport in proton conductors for fuel-cell applications: simulations, elementary reactions, and phenomenology. *Chem. Rev.* **104,** 4637–4678 (2004).
14. Mauritz, K. A. & Moore, R. B. State of understanding of Nafion. *Chem. Rev.* **104,** 4535–4385 (2004).
15. Norby, T. Proton conduction in solids: bulk and interfaces. *MRS Bull.* **34,** 923–928 (2009).
16. Fabbri, E., Pergolesi, D. & Traversa, E. Materials challenges toward proton-conducting oxide fuel cells: a critical review. *Chem. Soc. Rev.* **39,** 4355–4369 (2010).
17. Yoon, M., Suh, K., Natarajan, S. & Kim, K. Proton conduction in metal–organic frameworks and related modularly built porous solids. *Angew. Chem. Int. Ed.* **52,** 2688–2700 (2013).
18. Grotthuss, C. J. T. de. Sur la décomposition de l'eau et des corps qu'elle tient en dissolution à l'aide de l'électricité galvanique. *Ann. Chim.* **58,** 54–73 (1806).
19. Agmon, N. The Grotthuss mechanism. *Chem. Phys. Lett.* **244,** 456–462 (1995).
20. Cukierman, S. Et tu Grotthuss! and other unfinished stories. *Biochim. Biophys. Acta* **1757,** 876–885 (2006).
21. Algie, J. E., Downes, J. G. & Mackay, B. H. Electrical conduction in keratin. *Text. Res. J.* **30,** 432–434 (1960).
22. Bardelmeyer, G. H. Electrical conductivity in hydrated collagen. I. Conductivity mechanisms. *Biopolymers* **12,** 2289–2302 (1973).
23. Murphy, E. J. Ionic conduction in keratin (wool). *J. Colloid Interface Sci.* **54,** 400–408 (1976).
24. Tredgold, R. H., Sproule, R. C. & McCanny, J. Proton conduction in protein films. *J. Chem. Soc. Faraday Trans. 1* **72,** 509–512 (1976).
25. Careri, G., Geraci, M., Giasanti, A. & Rupley, J. A. Protonic conductivity of hydrated lysozyme powders at megahertz frequencies. *Proc. Natl Acad. Sci. USA* **82,** 5342–5346 (1985).
26. Gabriel, B. & Teissie, J. Proton long-range migration along protein monolayers and its consequence on membrane coupling. *Proc. Natl Acad. Sci. USA* **93,** 14521–14525 (1996).
27. Kaplan, D. & McGrath, K. *Protein-Based Materials – Bioengineering of Materials* (Birkhäuser, 1996).
28. Maskarinec, S. A. & Tirrell, D. A. Protein engineering approaches to biomaterials design. *Curr. Opin. Biotechnol.* **16,** 422–426 (2005).
29. Shen, L., Bao, N., Zhou, Z., Prevelige, P. E. & Gupta, A. Materials design using genetically engineered proteins. *J. Mater. Chem.* **21,** 18868–18876 (2011).
30. DiMarco, R. L. & Heilshorn, S. C. Multifunctional materials through modular protein engineering. *Adv. Mater.* **24,** 3923–3940 (2012).
31. Grove, T. Z. & Regan, L. New materials from proteins and peptides. *Curr. Opin. Struct. Biol.* **22,** 451–456 (2012).
32. Owens, R. M. & Malliaras, G. G. Organic electronics at the interface with biology. *MRS Bull.* **35,** 449–456 (2010).
33. Svennersten, K., Larsson, K. C., Berggren, M. & Richter–Dahlfors, A. Organic bioelectronics in nanomedicine. *Biochim. Biophys. Acta* **1810,** 276–285 (2011).
34. Tarabella, G. *et al.* New opportunities for organic electronics and bioelectronics: ions in action. *Chem. Sci.* **4,** 1395–1409 (2013).
35. Glowacki, E. D., Irimia-Vladu, M., Bauer, S. & Sariciftci, N. S. Hydrogen-bonds in molecular solids – from biological systems to organic electronics. *J. Mater. Chem. B* **1,** 3742–3753 (2013).
36. Meredith, P., Bettinger, C. J., Irimia-Vladu, M., Mostert, A. B. & Schwenn, P. E. Electronic and optoelectronic materials and devices inspired by nature. *Rep. Prog. Phys.* **76,** 034501 (2013).
37. Petrenko, V. F. & Maeno, N. Ice field transistor. *J. Phys. Colloq.* **48,** 115–119 (1987).
38. Chiragwandi, Z. G., Nur, O., Willander, M. & Calander, N. DC characteristics of a nanoscale water-based transistor. *Appl. Phys. Lett.* **83,** 5310–5312 (2003).
39. Fan, R., Huh, S., Yan, R., Arnold, J. & Yang, P. Gated proton transport in aligned mesoporous silica films. *Nature Mater.* **7,** 303–307 (2008).
40. Zhong, C. *et al.* A polysaccharide bioprotonic field-effect transistor. *Nature Commun.* **2,** 476 (2011).
41. Deng, Y. *et al.* H^+-type and OH^--type biological protonic semiconductors and complementary devices. *Sci. Rep.* **3,** 2481 (2013).
42. Deml, A. M., Bunge, A. L., Reznikov, M. A., Kolessov, A. & O'Hayre, R. P. Progress toward a solid-state ionic field effect transistor. *J. Appl. Phys.* **111,** 074511 (2012).
43. Crookes, W. J. *et al.* Reflectins: the unusual proteins of squid reflective tissues. *Science* **303,** 235–238 (2004).
44. Kramer, R. M., Crookes-Goodson, W. J. & Naik, R. R. The self-organizing properties of squid reflectin protein. *Nature Mater.* **6,** 533–538 (2007).
45. Tao, A. R. *et al.* The role of protein in assembly in dynamically tunable bio-optical tissues. *Biomaterials* **31,** 793–801 (2010).
46. Izumi, M. *et al.* Changes in reflectin protein phosphorylation are associated with dynamic iridescence in squid. *J. R. Soc. Interface* **7,** 549–560 (2010).
47. Phan, L. *et al.* Reconfigurable infrared camouflage coatings from a cephalopod protein. *Adv. Mater.* **25,** 5621–5625 (2013).
48. Mäthger, L. M., Denton, E. J., Marshall, N. J. & Hanlon, R. T. Mechanisms and behavioural functions of structural coloration in cephalopods. *J. R. Soc. Interface* **6,** 149–163 (2009).
49. DeMartini, D. G., Krogstad, D. V. & Morse, D. E. Membrane invaginations facilitate reversible water flux driving tunable iridescence in a dynamic biophotonic system. *Proc. Natl Acad. Sci. USA* **110,** 2552–2556 (2013).
50. Wardill, T. J., Gonzalez-Bellido, P. T., Crook, R. J. & Hanlon, R. T. Neural control of tunable skin iridescence in squid. *Proc. R. Soc. B* **279,** 4243–4252 (2012).
51. Ursúa, A., Gandía, L. M. & Sanchis, P. Hydrogen production from water electrolysis: current status and future trends. *Proc. IEEE* **100,** 410–426 (2012).
52. Zeng, K. & Zhang, D. Recent progress in alkaline water electrolysis for hydrogen production and applications. *Prog. Energy Combust. Sci.* **36,** 307–326 (2010).
53. Glasser, L. Proton conduction and injection in solids. *Chem. Rev.* **75,** 21–65 (1975).
54. Cordes, M. & Giese, B. Electron transfer in peptides and proteins. *Chem. Soc. Rev.* **38,** 892–901 (2009).
55. Shinwari, M. W., Deen, M. J., Starikov, E. B. & Cuniberti, G. Electrical conductance in biological molecules. *Adv. Funct. Mater.* **20,** 1865–1883 (2010).
56. Ron, I., Pecht, I., Sheves, M. & Cahen, D. Proteins as solid-state electronic conductors. *Acc. Chem. Res.* **43,** 945–953 (2010).
57. Winkler, J. R. & Gray, H. B. Long-range electron tunneling. *J. Am. Chem. Soc.* **136,** 2930–2939 (2014).
58. Barsoukov, E. & Macdonald, J. R. *Impedance Spectroscopy: Theory, Experiment and Applications* 2nd edn (Wiley, 2005).
59. Yuan, X-Z., Song, C., Wang, H. & Zhang, J. *Electrochemical Impedance Spectroscopy in PEM Fuel Cells: Fundamentals and Applications* (Springer, 2012).
60. Huggins, R. A. Simple method to determine electronic and ionic components of the conductivity in mixed conductors: a review. *Ionics* **8,** 300–313 (2002).
61. Xie, Z. *et al.* Discrepancies in the measurement of ionic conductivity of PEMs using two- and four-probe AC impedance spectroscopy. *J. Electrochem. Soc.* **153,** 173–178 (2006).
62. Soboleva, T. *et al.* Investigation of the through-plane impedance technique for evaluation of anisotropy of proton conducting polymer membranes. *J. Electroanal. Chem.* **622,** 145–152 (2008).
63. Morgan, H., Pethig, R. & Stevens, G. T. A proton-injecting technique for the measurement of hydration-dependent protonic conductivity. *J. Phys. E* **19,** 80–82 (1986).
64. Creighton, T. E. *Proteins: Structures and Molecular Properties* 2nd edn (W. H. Freeman, 1993).
65. Stavrinidou, E. *et al.* Direct measurement of ion mobility in a conducting polymer. *Adv. Mater.* **25,** 4488–4493 (2013).

Acknowledgements

We thank S. Hess at the California Institute of Technology Proteome Exploration Laboratory for assistance with the tryptic digestion and mass spectrometry experiments. We thank Professor Albert Yee's Laboratory for the use of their optical microscope. We thank J. Angle in Professor Martha Mecartney's Laboratory for the use of custom-built EIS equipment during the temperature-dependent measurements and S. Yang in Professor John Kymissis' Laboratory for the use of EIS equipment during the deuterium oxide measurements. We thank the Penner and Law Laboratories for the use of their atomic force microscope. We also thank P. Sheehan and the Naval Research Laboratory and Professor Zhibin Guan's Laboratory for the use of their thermogravimetric analysis instruments. A.A.G. acknowledges the Air Force Office of Scientific Research (FA9550-14-1-0144) and the University of California, Irvine, for financial support. W.G.W. acknowledges the National Science Foundation Postdoctoral Research Fellowship in Biology (DBI1306188) for financial support.

Author contributions

Experiments were conceived by D.D.O. and A.A.G. Experiments were carried out by D.D.O., L.P., E.K., J-M.J. and N.H. Biological samples were produced by L.P. and W.G.W. The manuscript was written by A.A.G., D.D.O., L.P. and W.G.W.

Additional information

Supplementary information is available in the online version of the paper. Reprints and permissions information is available online at www.nature.com/reprints. Correspondence and requests for materials should be addressed to A.A.G.

Competing financial interests

The authors declare no competing financial interests.